# Journal Name

## ARTICLE

### Stretchable, adhesive and ultra-conformable elastomer thin films

Nobutaka Sato,[a] Atsushi Murata,[b] Toshinori Fujie[*cd] and Shinji Takeoka[*a]

Thermoplastic elastomers are attractive materials because of the drastic changes in their physical properties above and below the glass transition temperature ($Tg$). In this paper, we report that free-standing polystyrene (PS, $Tg$: 100$^o$C) and polystyrene-polybutadiene-polystyrene triblock copolymer (SBS, $Tg$: -70$^o$C) thin films with a thickness of hundreds of nanometers were prepared by a gravure-coating method. From the mechanical properties of those thin films characterized by a bulge test and a tensile test, the SBS thin films showed a much lower elastic modulus (ca. 0.045 GPa, 212 nm thickness) compared with the PS thin films (ca. 1.19 GPa, 217 nm thickness). The lower elastic modulus and lower thickness of the SBS thin films resulted in higher conformability and thus higher adhesive strength to an uneven surface such as an artificial skin model with roughness (Ra = 10.6 μm), even though they both have similar surface energies. By analyzing the mechanical properties of the SBS thin films, the elastic modulus and thickness of the thin film strongly correlated with the conformability to a rough surface, which then leads to a high adhesive strength. Therefore, the SBS thin film will be useful as coating layer for variety of materials.

## 1. Introduction

Elastomers are attractive materials for the biomedical, electronic and coating fields[1-9] due to their unique properties including elasticity, flexibility, and toughness. Those physical properties were key factors in the choice of materials used in electronic devices[1,8,9], self-healing materials[10-12], and wearable devices[4,13]. Elastomers show the characteristic of elongation to external forces instead of breakup; for instance, chewing gum changes its form to conform the substrate of teeth. The physical properties of the constituent polymer chains change from glassy to rubbery states at the glass transition temperature $(T_g)$[14,15]. Generally, polymers show glassy properties (rigid and fragile) below $T_g$ and rubbery properties (flexible and conformable) above $T_g$, while elastomers show reversible deformation under external force. Elastomers having those mechanical properties are generally classified into vulcanized rubbers and thermoplastic elastomers (TPEs).

TPEs are composed of soft segments of flexible rubbers and hard segments of rigid resins to prevent plastic deformation.

Polymeric ultra-thin films (formed as a nanosheet) are expected to be valuable for a wide variety of applications such as the electrochemical, biomedical, and printing fields[16-19]. Polymer nanosheets have unique properties, including thickness-dependent glass transition temperatures[20,21], and Young's moduli[22-24]. Understanding those physical and mechanical properties of the nanosheets allow us to control various functions such as adhesion and the molecular permeability of the nanosheets[25]. In particular, the adhesion property of the nanosheets is one of the fundamental characteristics for application of nanosheets onto various surfaces. Such nanosheets were able to attach to silicon wafers or organs, including skin and lung, without chemical glues[26-28]. So far, we have reported the unique mechanical properties of the nanosheets that consist of non-elastomer polyesters[22] and polyelectrolytes[28] by a bulge test and a micro-scratch test[29]. Interestingly, the adhesive force is increased with lowering the thickness to less than ca. 100 nm, which would be due to the high conformability of thinner nanosheets that would increase the total secondary interaction forces between the nanosheet and an adherend with some roughness. Although those nanosheets showed an enhancement of adhesion depending on the thickness, other factors such as flexibility and surface energy also have large association with the adhesion. In particular, the flexibility is an important factor that affects the adhesive strength on irregularly shaped surfaces. In previous studies, a poly(dimethylsiloxane) (PDMS) nanomembrane displayed high flexibility[30,31], but the PDMS nanomembrane was not suitable for large scale fabrication because a heat curing process for hours is essential for the PDMS pre-polymer. Therefore, we focused our attention on more appropriate

a. *Department of Life Science and Medical Bioscience, Graduate School of Advanced Science and Engineering, Waseda University, TWIns, 2-2 Wakamtsu-cho, Shinjuku-ku, Tokyo, 162-8480 (Japan).*
b. *Institute for Nanoscience and Nanotechnology, Waseda University, 513 Waseda Tsurumaki-cho, Shinjuku, Tokyo 162-0041 (Japan).*
c. *Waseda Institute for Advanced Study, Waseda University, TWIns, 2-2 Wakamatsu-cho, Shinjuku-ku, Tokyo, 162-8480 (Japan).*
d. *Japan Science and Technology Agency, PRESTO, 4-1-8 Honcho, Kawaguchi, Saitama, 332-0012 (Japan).*
e. *To whom correspondence: T.F. (t.fujie@aoni.waseda.jp) and S.T. (takeoka@waseda.jp).*
Electronic Supplementary Information (ESI) available: [Figures and tables showing supplier information of the tape test, mechanical properties of the PS and SBS thin films by the bulge test and tensile test, static contact angle of the PS and SBS thin films, and optical property of the SBS thin film with a thickness of 690 nm using an ultraviolet-visible absorption spectrophotometer. Movies showing stretching of the 212 nm-thick SBS thin film, elongation of the 690 nm-thick SBS thin film by the tensile tester, and the shatterproof experiments.]. See DOI: 10.1039/x0xx00000x

Soft Matter Accepted Manuscript

elastomers for the fabrication of thin films on large scale fabrication. Elastomer thin films with the thickness of more than 100 nm are expected to have both the mechanical properties of a bulk elastomer and the physical properties of conventional non-elastomer nanosheets with the thickness of ca. 100 nm. Understanding the unique physical properties of elastomer thin films compared with non-elastomer thin films is a necessary advance in nanomaterial fields.

In this study, we fabricated highly flexible and stretchable elastomer thin films and evaluated their mechanical and adhesive properties by a bulge test, a tensile test, and a cross-cut test according to ISO 2409 in comparison to a standard polymer (PS) thin film. These thin films were prepared by a micro-gravure coating method[18] and were simply detached from the polyethylene terephthalate (PET) substrate of using a water-soluble sacrificial layer of polyvinyl alcohol (PVA). Free-standing thin films were transferred to a silicon wafer or an artificial skin model to characterize the surface morphology, conformability and adhesive properties. Furthermore, the high adhesion and flexibility of those elastomer thin films showed mechanical durability by utilizing a shatterproof experiment.

## 2. Experiment

### Materials

Silicon wafers were purchased from KST World Co. (Fukui, Japan). The silicon wafers were cut into 2 cm × 2 cm pieces and immersed in a piranha solution ($H_2SO_4/H_2O_2$ = 3/1, v/v) at 120$^o$C for 15 min, followed by being thoroughly rinsed with deionized water (18 M$\Omega$ cm) to remove any contaminants adsorbed on the surface. Artificial skin models (Bioskin®, Beaulax Co., Ltd., Saitama, Japan) made from polyurethane were used in SEM observation and a tape test. This artificial skin model has been used in the field of cosmetics or coating materials[32-34]. It imitates the mechanical properties such as elastic modulus and roughness of stratum corneum of human skin; 0.95 MPa in the tensile strength, 480 % in the elongation, and 10.6 $\mu$m in the roughness ($R_a$). All organic solvents (reagent grade) and poly(vinyl alcohol) (PVA; $M_w$ 22 000, 86.5 - 89% hydrolyzed) were purchased from Kanto Chemical Co., Inc. (Tokyo, Japan) and used without purification. Polystyrene-block-polybutadiene-block-polystyrene (SBS; $M_w$ 140 000) and polystyrene (PS; $M_w$ 280 000) was purchased from Sigma-Aldrich Japan (Tokyo, Japan). IR and $^1$H-NMR spectra of SBS were measured and shown in Fig. S1. The monomer ratio of styrene and butadiene was 1 to 6.8 (butadiene 87 mol%) by calculating from the integral values attributed to styrene and butadiene in the $^1$H-NMR spectrum. The thickness of thin films was evaluated by AFM (VN-8000, KEYENCE Co., Ltd., Osaka, Japan).

### Preparation of PS and SBS thin films by gravure coating

Both PS and SBS thin films were fabricated by a microgravure technique utilizing a Mini-Lab coater (Yasui Seiki Co., Ltd., Kanagawa, Japan). The thickness of the thin films was controlled by the concentration of the polymer solution. A 2

wt% PVA solution was coated on a PET film (12 cm width, Lumirror® 25T60, Toray Industries Inc., Tokyo, Japan) with a rotation speed of the gravure roll at 30 rpm, a line speed of 1.3 m/min and a drying temperature of 100$^o$C. SBS and PS were dissolved in tetrahydrofuran (THF) and ethyl acetate, respectively. After filtration with a syringe filter (Supra Pure®, 0.2 $\mu$m, Recenttec Inc.), those polymer solutions were coated on the PVA/PET films under the same conditions as PVA coating, except for the use of an 80$^o$C drying temperature. The resulting polymeric thin film was released from the PET substrate by water immersion to dissolve the sacrificial PVA layer. In measuring thickness of PS and SBS thin films, first, both edges of the PS or SBS coated on PET films (1 m in the length and 12 cm in the width) were trimmed down about 1 cm. Next, three areas from this film were randomly selected, cut into pieces, and then transferred to silicon wafers. The average thickness and standard deviation of each polymer thin film were calculated from three places of each piece by AFM.

### AFM observations of thin films on a silicon wafer

Atomic force microscopy (AFM, Innova SPM, BRUKER Co., Ltd., MA, USA) was used to investigate the surface morphologies and to perform the surface analyses of the PS and SBS thin films on silicon wafers. AFM measurements were carried out with a piezoscanner (maximum scan size 50 $\mu$m × 50 $\mu$m) at room temperature. Commercially available cantilever-style tapping mode tips (RTESPA-CP, Silicon AFM Probes, BRUKER Co., Ltd.) were used, with a resonance frequency in the range of 290 - 330 kHz. AFM tapping phase images were filtered and analyzed by the analysis software NanoScope Analysis (BRUKER).

### SEM observation of the thin films on an artificial skin model films

The surface morphologies of the PS and SBS thin films on an artificial skin model ($R_a$ = 10.6±1.8 $\mu$m) were evaluated by SEM (VE-9800, KEYENCE Co., Ltd., Osaka, Japan). The thin films were transferred on the artificial skin model from a free-standing state on an air-water interface using a mesh.

### Measurement of contact angle

Free-standing PS and SBS thin films were transferred on a silicon wafer and dried *in vacuo*. Then, 4 $\mu$L of MilliQ water was dropped onto the thin film and the contact angle was measured within 30 sec after the droplet deposition. Young's equation (1) described the principle of the contact angle[35].

$$\gamma_s = \gamma_{sl} + \gamma_l \cos \vartheta \qquad (1)$$

Here, $\vartheta$, $\gamma_s$, $\gamma_l$, and $\gamma_{sl}$ represent the contact angle, the solid surface free energies, liquid surface free energies, solid-liquid interfacial energies, respectively.
The work of adhesion between a solid surface and liquid can be represented by equations (2) and (3)[36,37].

$$W_{sl} = \gamma_s + \gamma_l - \gamma_{sl} \qquad (2)$$

**ARTICLE**

eq. (1) and eq. (2) are combined, resulting in eq. (3)

$$W_{sl} = \gamma_l (1 + \cos \theta) \qquad (3)$$

### Analysis of mechanical properties of thin films by a bulge test

A bulge test was performed as described in the previous studies[38,39,40]. In order to determine the ultimate tensile strength and elastic modulus of thin film, the following equations were used.

$$\sigma = \frac{P \cdot a \cdot u}{a \cdot a \cdot a \cdot a} \qquad (4)$$

$$\varepsilon = \frac{a \cdot A \cdot u}{a \cdot a \cdot a} \qquad (5)$$

$$E = \frac{\sigma}{\varepsilon} \qquad (6)$$

Here, $\sigma$, $P$, $a$, $h$, $d$, $\varepsilon$ and $E$ represent tensile stress, applied pressure, the radius of the circular hole of the steel plate, thickness, deflection, tensile strain, and elastic modulus of the thin film, respectively.

### Analysis of mechanical properties of thin films by a tensile test

A tensile test of the PS and SBS thin films was performed at $23\pm2^{\circ}C$ and $50\pm5\%$ humidity using a tensile tester (EZ-S-5 N, SHIMADZU Co., Ltd., Kyoto, Japan) with a tensile speed of 10 mm/min, according to ISO 3270. Mechanical data such as normal stress and normal strain were calculated by the analysis software TRAPEZIUM X (SHIMADZU). From the stress-strain curves, the tensile strength, elongation and Young's modulus (strain 2.5 - 5%) of the thin films were calculated.

### Shatterproof experiment

PS and SBS thin films with thickness of 697 nm and 690 nm were attached to cover glasses (22 mm × 22 mm, thickness 0.12 - 0.17 mm, Matsunami Glass Co., Ltd., Osaka, Japan), respectively. Prior to the shatterproofing experiment, the glass substrates were set in an environmental chamber for 24 hrs (temperature 23°C, humidity 50%). Then, the substrates were smashed by a house-hold hammer (head weight: 57 g).

### Measurement of adhesive strength of thin films on an artificial skin model by a tape test

The adhesive strength of the PS and SBS thin films on the artificial skin model was evaluated by a tape test according to the ISO 2409. The temperature and humidity were controlled by an environmental chamber (KCL-2000A, Tokyo Rikakikai Co., Ltd., Tokyo, Japan) as $32\pm2^{\circ}C$ and $50\pm5\%$ in accord with ISO 3270. The thin films were transferred on to the artificial skin model from a free-standing state on an air-water interface by using a mesh. These thin films were peeled off from the artificial skin model by using a standard tape (Cellophane tape CT-24, Nichiban Co., Ltd., Tokyo, Japan) with an adhesive strength of 4.0 N/cm and other tapes having different adhesive strengths from 0.08 to 4.0 N/cm (Table S1). The data were classified by a number from 0 to 5, depending on the size of the detachment area. The detachment area used, more than 65%, 35 - 65 %, 15 - 35 %, 5 - 15%, less than 5%, and 0% were classified as 5, 4, 3, 2, 1, and 0, respectively. The adhesive strength of each tape was determined according to the ISO 29862-29864.

## 3. Results and discussion

PS and SBS thin films were fabricated by a micro-gravure coating method on a PVA-coated PET film. After gradually detaching those thin films from the PET substrate by dissolving the PVA layer in water, the resulting free-standing thin film floating at an air-water interface, as shown in Fig. 1a, could be easily scooped onto a silicon wafer for a thickness measurement. The SBS thin film with the thickness of 690 nm was stretchable as shown in Fig. 1b. The PS thin films fabricated from 2, 2.5, and 7 wt% ethyl acetate solutions had thicknesses of $127\pm10$ nm, $217\pm5$ nm and $697\pm7$ nm, respectively, whereas the thicknesses of SBS thin films fabricated from 1, 2, 2.5, and 4 wt% tetrahydrofuran (THF) solutions are shown in Fig. 1c. As predicted from the data of the PS thin films, the thickness of the SBS thin films depends on the concentration of the SBS solution. Those average thicknesses were used for a bulge test and a tensile test.
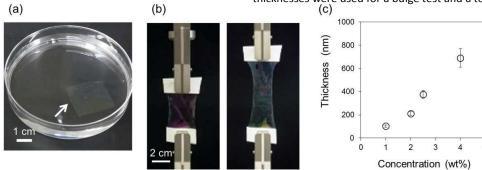


**Fig. 1** Membrane stability on water and thickness control of SBS thin films (a) Free-standing 212 nm-thick SBS thin film (white arrow, 2 cm × 2 cm) on an air-water interface. (b) Free-standing 690 nm-thick SBS thin film stretched by a tensile tester. (c) Relationship between the concentration of the SBS THF solution and the thickness of the resulting SBS thin films.

As shown in Tables 1 and 2, we prepared five samples and evaluated them; PS thin films with the thickness of 127 nm (conventional nanosheet), 217 nm, and 697 nm thickness were used as standard samples, and SBS thin films with similar thickness to the two thicker PS films, one with 212 nm thickness (thinner SBS thin film) and one with 690 nm thickness (thicker SBS thin film) were compared to the three PS thin films. The movie S1 (shown in Supporting Information) demonstrates the stretchable nature of the 212 nm SBS film; it could be stretched with tweezers from 1 cm to ca. 3 cm and returned back to the original size after being released from the tweezers. However, the 217 nm PS film could not be stretched but broken under the same treatment. Thus, the PS thin film was not able to sustain a self-supporting state in air.

Next, the surface morphology and wettability of the PS and SBS thin films were observed, as shown in Fig. 2 and S2. First, the surface morphology of the 217 and 697 nm PS films and the 212 and 690 nm SBS films on silicon wafers were observed by atomic force microscopy (Fig. 2a - d). The 212 and 690 nm SBS films were stretched (100% tensile elongation) by a tensile tester and then transferred onto silicon wafers (Fig. 2e, f). The surface of the 217 nm PS film was flat (Fig. 2a), whereas that of the 697 nm PS film was phase-separated due to supersaturation and the average diameter of polystyrene domains were about 150 nm (Fig. 2b). On the other hand, the SBS thin films were phase-separated into polystyrene and polybutadiene domains (Fig. 2c, d). In previous studies[41,42,43], the surfaces of a SBS thin film adopted various phase-separated structures consisting of polystyrene cylinders and/or spheres in a polybutadiene matrix. According to the tapping phase images and the above previous studies, the bright domains and dark domains are attributed to polystyrene and polybutadiene, respectively. Polystyrene domains in the 212 nm SBS film were larger than those of the 690 nm. Therefore, polystyrene domains would easily aggregate when the thinner SBS films were fabricated in the polymer solution (20 mg/mL) with a lower viscosity. The thickness of films depended on the concentration of the polymer solutions; the thin films were fabricated from the low concentration polymer solutions. Furthermore, orientation of styrene domains was observed in the surface of elongated SBS thin films with thicknesses of 212 nm and 690 nm (Fig. 2e, f).

The wettability of thin films was evaluated by a contact angle measurement using a droplet of MilliQ water (Fig. S2). The static contact angles of the 127 nm, 217 nm, and 697 nm PS films, and the 212 and 690 nm SBS films were 77±2°, 76±1°, 78±2°, 82±1°, and 83±1°, respectively. In addition, the static contact angle of an artificial skin model was 114±3°. The adhesion energy of these thin films is shown in Table S3 in the Supporting Information. In general, although wettability is a critical factor for adhesion, this table indicated that the wettability of PS and SBS thin film were much the same. Therefore, wettability would not be a factor for adhesive strength of these thin films to the artificial skin model. The conformability of PS and SBS thin films on an artificial skin model was examined by SEM (Fig. 3).
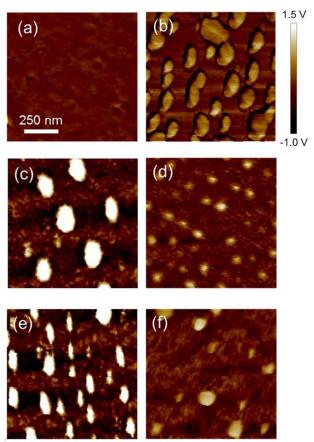


**Fig. 2** (a) - (d) AFM images of PS thin film with thicknesses of 217 nm (a) and 697 nm (b) and SBS thin film with thicknesses of 212 nm (c) and 690 nm (d). SBS thin films with thicknesses of 212 nm (e) and 690 nm (f) which were elongated (elongation ratio was 100%) by using a tensile tester.

The 127, 217, and 697 nm PS films, and the 212 and 690 nm SBS films on the artificial skin models are shown in Fig. 3a - e, respectively. The thinnest PS film (127 nm) showed the most conformable nature to the rough surface (Fig. 3a, b, and c). In addition, the thinner SBS film (212 nm, Fig. 3d) was more conformable than the thicker one (690 nm, Fig. 3e). Thus, it is indicated that the conformability to the rough surface depended on the thickness of the thin films. Furthermore, the 217 nm PS film did not conform to the rough surface (Fig. 3b), whereas the 212 nm SBS film clearly conformed to the rough surface and the boundary line between the SBS thin film and artificial skin model was obscure (Fig. 3d). Similarly, the thicker 690 nm SBS film was much more conformable than the similar thickness 697 nm PS thin film. These results indicated that the shape-following ability of the thin film was dependent on its thickness and the kind of polymer; in this case, the presence of rich butadiene component (87 mol% of butadiene units) in the polymer chain. Some mechanical properties of the thin film were studied by a bulge test. Cross-sectional views of the deflection of four thin film samples at 0.2 - 0.8 kPa pressures are shown in Fig. S3 in the Supporting Information, and those at a
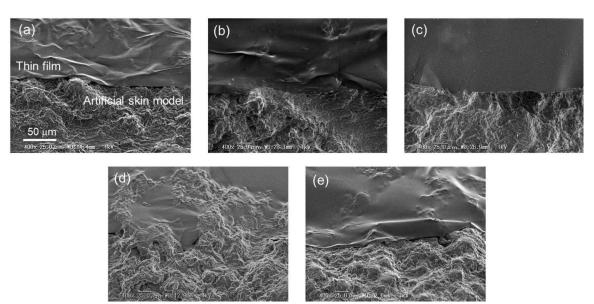
**Fig. 3** SEM images at the edge of the PS (a), (b), and (c), and SBS (d) and (e) thin films on an artificial skin model ($Ra$ = 10.6 μm). Thickness of these thin films was (a) 127 nm, (b) 217 nm, (c) 697 nm, (d) 212 nm, and (e) 690 nm.

0.8 kPa pressure are representatively shown in Fig. 4a. The 212 nm SBS film was highly deflected as compared to the 217 nm PS film with the similar thickness. It showed a larger deflection than the 690 nm SBS film, and even the 690 nm SBS film showed a larger deflection than the thinnest PS film (127 nm). The ultimate tensile strength and the elastic modulus of each thin film were calculated as described in the experimental section (eq. (4) – eq. (6)). Pressure-deflection curves of the four PS and SBS thin films are shown in Fig. 4b. The slope of the curve indicated that the SBS films were deflected in the lower pressure regions compared with the PS films, and the thinner SBS film showed the higher rate of deflection at the same pressure than the thicker one. These pressure-deflection curves were converted into stress-strain curves (Fig. 4c), and the ultimate tensile strength, ultimate tensile elongation, and elastic modulus were calculated from the initial elasticity of the stress-strain curve for each thin film and were listed in Table 1. The elastic moduli of the thinner and thicker SBS film were 0.045±0.025 GPa and 0.059±0.026 GPa, respectively. Thus, the thinner and thicker SBS films have a similar elastic modulus in each case.

**Table 1** Mechanical properties of the PS and SBS thin films with different thicknesses evaluated by a bulge test

| Polymer | Thickness (nm) | Ultimate tensile strength (MPa) | Ultimate tensile elongation (%) | Elastic modulus (GPa) |
|---------|----------------|----------------------------------|----------------------------------|------------------------|
| PS | 127±10 | 16±3 | 6.3±2.4 | 0.90±0.05 |
| PS | 217±5 | 16±3 | 4.4±1.1 | 1.19±0.33 |
| SBS | 212±16 | 1.4±0.2 | 18.2±5.1 | 0.045±0.025 |
| SBS | 690±79 | 1.2±0.3 | 19.8±14.4 | 0.059±0.026 |

Owing to the presence of the butadiene part of the polymer chain, the 212 nm SBS film showed ca. 16 times lower ultimate tensile strength, ca. 4 times ultimate tensile elongation, and ca. 20 times lower elastic modulus compared to the 217 nm PS film. In a previous study about an elastomer thin film[39], polyurethane (PU) thin films were fabricated with crosslinking acryl urethane resin. The PU thin film showed 33.6 % in the elongation and 10 MPa in the tensile strength. On the other hand, the SBS thin film showed 20 % in the elongation and 1.3 MPa in the tensile strength, respectively. As these elastomers are consisted of soft and hard segments, employment of elastomers for the thin film fabrication allowed for the softening of thin films down to MPa order (i.e., soft and hard segments of PU are attributed to the alkyl chains of polyol and urethane domains, whereas those of SBS are attributed to the butadiene and styrene domains.). Additionally, in our previous studies[27,28], poly(L-lactic acid) (PLLA) thin films and polysaccharide thin films composed of chitosan and sodium alginate were fabricated. The elastic modulus of the 23 nm PLLA film and the 35 nm polysaccharide film were 1.7 GPa and 1.1 GPa, respectively. Thus, the elastic modulus of SBS thin film was much lower than that of those thin films in spite of it being more than 200 nm in thickness. Furthermore, considering the facts that elastic moduli of those films were GPa order, employing elastomers could contribute to reducing the elastic modulus from GPa to MPa.

In addition to the bulge test, the mechanical properties of the 212 and 690 nm SBS films and the 697 nm PS film were evaluated using a tensile tester. The behavior of the 690 nm SBS film under loading by the tensile tester is representatively shown in Movie S2 in the Supporting Information. The tensile strength, elongation, and Young's modulus of those thin films were calculated from the stress-strain curves produced from the tensile test (Fig. S4, Table S2). The tensile strength of the 697 nm PS film was 5.4 MPa, which was ca. 6 times higher than
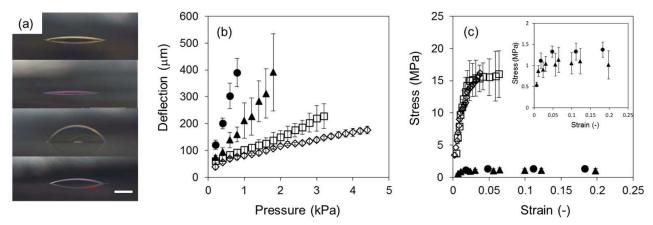
**Fig. 4** Evaluation of mechanical properties of the thin films. (a) Sequential cross-sectional views of deflection at 0.8 kPa pressure of the PS thin film with thicknesses of 127 nm and 217 nm, and the SBS thin films with thicknesses of 212 nm and 690 nm in order from the top. (n=3) scale bar : 500 $\mu$m (b) Pressure-deflection and (c) stress-strain curve of the PS thin film with thicknesses of 127 nm ($\square$) and 217 nm ($\diamond$) and SBS thin films with thicknesses of 212 nm ($\bullet$) and 690 nm ($\blacktriangle$). Inset shows magnified plots of the SBS thin films.

those of the thicker and thinner SBS films. Generally, the tensile strength of bulk PS and SBS are 45 ~ 60 MPa[44] and 2.5 ~ 30 MPa[45], respectively. As compared with bulk polymers, the values of 5.4 MPa of the PS thin film, and ca. 1 MPa of the SBS thin film were quite low. Elongation of the 697 nm PS film was 1.8 %, which was ca. 100 times lower than that of the 690 nm SBS film. The Young's modulus of the 697 nm PS film was 0.52 GPa, whereas those of the 212 and 690 nm SBS films were 5.7±1.2 MPa and 4.9±0.8 MPa, respectively. Thus, the SBS thin film showed a thickness-independent Young's modulus and much lower Young's modulus compared with the PS thin film with the similar thickness. These results indicated that the mechanical properties such as elastic modulus and Young's modulus strongly depended on the kinds of polymers used rather than the thickness of the thin film.

**Table 2** Adhesive strength scores of thin films on an artificial skin model evaluated by a cross-cut tape test. The detachment areas of more than 65%, 35-65%, 15-35%, 5-15%, less than 5%, and 0% were scored as 5, 4, 3, 2, 1, and 0, respectively

| Adhesive strength (N/cm) | PS 127 nm | PS 217 nm | PS 697 nm | SBS 212 nm | SBS 690 nm |
|---|---|---|---|---|---|
| 4.01 | 5 | 5 | 5 | 5 | 5 |
| 2.59 | - | - | - | 5 | - |
| 1.18 | - | - | - | 5 | - |
| 1.06 | - | - | - | 5 | - |
| 0.78 | - | - | - | 0 | 5 |
| 0.71 | - | - | - | - | 5 |
| 0.29 | 5 | - | - | - | 0 |
| 0.22 | 5 | - | - | 0 | 0 |
| 0.18 | 5 | - | - | - | - |
| 0.08 | 1 | 5 | 5 | - | - |

In addition, SEM observations (Fig. 3) demonstrated that the elastomer SBS thin films expanded and contracted at very low stress and conformed to the substrate with the rough surface because elastic modulus of the SBS thin film was ca. 20 times smaller than that of the PS thin film.

Next, the adhesive strength of those thin films was evaluated according to the cross-cut test described in ISO 2409 with scoring from 0 to 5 under strict control of the temperature (32°C) and humidity (50%) by using an environmental control chamber and a glove box. At first, an artificial skin model and Cellophane tape® were used as an adherend and a pressure-sensitive adhesive tape, respectively. All thin films were easily detached from the artificial skin model when using the Cellophane tape® with adhesive strength of 4.01 N/cm. Therefore, various tapes with different adhesive strengths lower than 4.01 N/cm were used for the cross-cut test, and the results were summarized in Table 2. The adhesive strengths of the 127 nm PS film, and the 212 and 690 nm SBS film were estimated as 0.08 - 0.18 N/cm, 0.78 - 1.06 N/cm, and 0.29 - 0.71 N/cm, respectively. Also, those of the 217 and 697 nm PS films were estimated as lower than 0.08 N/cm. Altogether, the 212 nm SBS film showed the highest adhesion and even the 690 nm SBS film had much larger adhesive strength than the thinnest PS film (127 nm). Therefore, it is suggested that the adhesive strength on the artificial skin model was influenced by the conformability of the thin films, which is related to the elastic modulus and thickness of the thin film.

Finally, the SBS thin films showed the mechanical durability by utilizing a shatterproof experiment. The 697 nm PS and 690 nm SBS films were attached to cover glasses (22 mm × 22 mm, thickness 0.12 - 0.17 mm) and set in the experimental chamber (temperature 23°C, humidity 50%) for 24 hrs. Then, a pristine cover glass and those samples were smashed by a hammer (Movie S3). In general, rubber and elastomers such as TPE and

silicon resin are used for shatterproof materials of window glasses and liquid crystal displays owing to their high elasticity for shock absorption. Pristine and PS thin film-attached cover glasses were scattered in all directions (Movie S3a, b), whereas the SBS thin film-attached cover glass was not scattered; the smashed glass was supported with the SBS thin film and then could be picked up with tweezers (Movie S3c). The adhesion of the SBS thin film to the glass was sufficiently strong in spite of its submicron thickness. The low elastic modulus of the SBS thin film is probably responsible for it preventing the cover glass scattering. These results suggested that the SBS thin film could be used for coating materials. The transmittance of the 690 nm SBS film was approximately 100% in the wavelength region from 300 to 800 nm because of its submicron thickness (Fig. S5). Taken together, these results suggest that the SBS thin films are good candidates to be applicable as coating material to protect electronic devices.

## 4. Conclusions

We fabricated free-standing elastomer thin films made from SBS using a micro-gravure coating method. The mechanical and adhesion properties of the elastomer SBS and standard polymer PS thin films were compared in this study. The SBS thin films showed a much lower elastic modulus and a higher adhesive strength compared to PS films with a similar thickness owing to the presence of the butadiene part of the polymer chain. Though the elastic modulus of the SBS thin films did not depend on the thickness, the thinner SBS films were more conformable and had larger adhesive strengths than the thicker SBS films. Therefore, the elastic modulus and thickness appear to correlate with the conformability to a rough surface, which then determines the adhesive strength. These results indicate that the adhesive strength is controllable by the elastic modulus and thickness rather than the free energy, as both SBS and PS have similar free energies. The SBS thin films with high mechanical stability are adhered to the rough surfaces and have a high probability of acting as excellent coating materials.
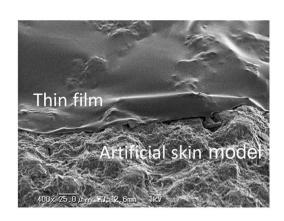
## Acknowledgements

## Notes and references

1   D.-H. Kim, J.-H. Ahn, W. M. Choi, H. Kim, T. Kim, J. Song, Y. Y. Huang, Z. Liu, C. Lu and J. A. Rogers, *Science*, 2008, **320**, 507-511.
2   S.-I. Park, Y. Xiong, R.-H. Kim, P. Elvikis, M. Meitl, D.-H. Kim, J. Wu, J. Yoon, C.-J. Yu, Z. Liu, Y. Huang, K.-C. Hwang, P. Ferreira, X. Li, K. Choquette and J. A. Rogers, *Science*, 2009, **325**, 977-981.
3   Y. Wang, G. A. Ameer, B. J. Sheppard and R. Langer, *Nat. Biotechnol*ogy, 2002, **20**, 602-606.
4   G. S. Jeong, D.-H. Baek, H. C. Jung, J. H. Song, J. H. Moon, S. W. Hong, I. Y. Kim and S.-H. Lee, *Nat. Commun.*, 2012, **3**, 977.
5   C. L. E. Nijst, J. P. Bruggeman, J. M. Karp, L. Ferreira, A. Zumbuehl, C. J. Bettinger and R. Langer, *Biomacromolecules*, 2007, **8**, 3067-3073.
6   G. C. E. Jr, M. Cheng, C. J. Bettinger, J. T. Borenstein, R. Langer and L. E. Freed, *Nat. Mater.*, 2008, **7**, 1003-1010.
7   B. Yu, S.-Y. Kang, A. Akthakul, N. Ramadurai, M. Pilkenton, A. Patel, A. Nashat, D. G. Anderson, F. H. Sakamoto, B. A. Gilchrest, R. R. Anderson and R. Langer, *Nat. Mater.*, 2016, **15**, 911–918.
8   J. Liang, L. Li, X. Niu, Z. Yu and Q. Pei, *Nat. Photonics*, 2013, **7**, 817-824.
9   C. Larson, B. Peele, S. Li, S. Robinson, M. Totaro, L. Beccai, B. Mazzolai and R. Shepherd, *Science*, 2016, **351**, 1071-1074.
10  L. Zhu and R. P. Wool, *Polymer*, 2006, **47**, 8106-8115.
11  D. A. Davis, A. Hamilton, J. Yang, L. D. Cremar, D. V. Gough, S. L. Potisek, M. T. Ong, P. V. Braun, T. J. Martínez, S. R. White, J. S. Moore and N. R. Sottos, *Nature*, 2009, **459**, 68-72.
12  Y. Chen, A. M. Kushner, G. A. Williams and Z. Guan, *Nat. Chem.*, 2012, **4**, 467-472.
13  S. Bauer, *Nat. Mater.*, 2013, **12**, 871–872.
14  J. A. Forrest and K. Dalnoki-Veress, *J. Polym. Sci., Part B: Polym. Phys.*, 2001, **39**, 2664-2670.
15  J. Perez and J. Y. Cavaillé, *J. Non-Cryst. Solids*, 1994, **172-174**, 1028-1036.
16  W. Cheng, M. J. Campolongo, S. J. Tan and D. Luo, *Nano Today*, 2009, **4**, 482-493.
17  R. R. Costa and J. F. Mano, *Chem. Soc. Rev.*, 2014, **43**, 3453-3479.
18  R. R. Sondergaard, M. Hosel and F. C. Krebs, *J. Polym. Sci., Part B: Polym. Phys.*, 2013, **51**, 16-34.
19  K. Ariga, Y. Yamauchi, G. Rydzek, Q. Ji, Y. Yonamine, K. C.-W. Wu and J. P. Hill, *Chem. Lett.*, 2014, **43**, 36-68.
20  J. L. Keddie, R. A. L. Jones and R. A. Cory, *Europhys. Lett.*, 1994, **27**, 59-64.
21  N. Satomi, A. Takahara and T. Kajiyama, *Macromolecules*, 1999, **32**, 4474-4476.
22  T. Fujie, L. Ricotti, A. Desii, A. Menciassi, P. Dario and V. Mattoli, *Langmuir*, 2011, **27**, 13173-13182.
23  C. M. Stafford, C. Harrison, K. L. Beers, A. Karim, E. J. Amis, M. R. Vanlandingham, H.-C. Kim, W. Volksen, R. D. Miller and E. E. Simonyi, *Nat. Mater.*, 2004, **3**, 545-550.
24  A. J. Nolte, R. E. Cohen and M. F. Rubner, *Macromolecules*, 2006, **39**, 4841-4847.
25  T. Fujie, Y. Kawamoto, H. Haniuda, A. Saito, K. Kabata, Y. Honda, E. Ohmori, T. Asahi and S. Takeoka, *Macromolecules*, 2013, **46**, 395-402.
26  T. Fujie, Y. Okamura and S. Takeoka, *Adv. Mater.*, 2007, **19**, 3549-3553.
27  Y. Okamura, K. Kabata, M. Kinoshita, D. Saitoh and S. Takeoka, *Adv. Mater.*, 2009, **21**, 4388-4392.
28  T. Fujie, N. Matsutani, M. Kinoshita, Y. Okamura, A. Saito and S. Takeoka, *Adv. Funct. Mater.*, 2009, **19**, 2560-2568.
29  N. Kyouno, D. Arai, K. Takeshita and S. Baba, *J. Adhesion Sci. Technol.*, 2009, **23**, 1973-1991.
30  E. Kang, J. Ryoo, G. S. Jeong, Y. Y. Choi, S. M. Jeong, J. Ju, S. Chung, S. Takayama and S.-H. Lee, *Adv. Mater.*, 2013, **25**, 2167-2173.
31  A. L. Thangawng, R. S. Ruoff, M. A. Swartz and M. R. Glucksberg, *Biomed. Microdevices*, 2007, **9**, 587-595.
32  N. Kitamura, J. Chim and N. Miki, *J. Micromech. Microeng.*, 2015, **25**, Number 2.

33 Y. Nishinaka, R. Jun, G.S. Prihandana and N. Miki, *Jpn. J. Appl. Phys.*, 2013, **52**, Number 6S.

34 N. Ikeda, K. Miyashita, R. Hikima and S. Tominaga, *Color Res. Appl.*, 2014, **39**, 45-55.

35 T. Young, *Trans. R. Soc.*, 1805, **95**, 65-87.

36 S. Zhandarov and E. Mäder, *Compos. Interfaces*, 2003, **10**, 41-59.

37 B. Bouali, F. Ganachaud, J.-P. Chapel, C. Pichot and P. Lanteri, *J. Colloid Interface Sci.*, 1998, **208**, 81-89.

38 S. Markutsya, C. Jiang, Y. Pikus and V. V. Tsukruk, *Adv. Funct. Mater.*, 2005, **15**, 771-780.

39 H. Watanabe, T. Ohzono and T. Kunitake, *Macromolecules*, 2007, **40**, 1369-1371.

40 T. Fujie, S. Furutate, D. Niwa and S. Takeoka, *Soft matter*, 2010, **6**, 4672–4676.

41 C. Park, J. Yoon and E. L. Thomas, *Polymer*, 2003, **44**, 6725-6760.

42 L. Peponi, A. Tercjak, J. Gutierrez, H. Stadler, L. Torre, J. M. Kenny and I. Mondragon, *Macromol. Mater. Eng.*, 2008, **293**, 568-573.

43 Q. Zhang, O. K. C. Tsui, B. Du, F. Zhang, T. Tang and T. He, *Macromolecules*, 2000, **33**, 9561-9567.

44 Kagaku Binran Ouyokagakuhen, 7th ed., The Chemical Society of Japan Ed., Maruzen, Tokyo 2014, p.II-1137

45 Kagaku Binran Kisohen, 5th ed., The Chemical Society of Japan Ed., Maruzen, Tokyo 2004, p.I-721

*Stretchable*                    *Conformable*

156x77mm (300 x 300 DPI)